The Reduced Order Through-Flow Modeling of Axial Turbomachinery

Oleg DUBITSKY[1], Alexander WIEDERMANN[2],
Tsuguji NAKANO[1], John PERERA[1]

[1] Concepts NREC
217 Billings Farm Rd., White River Jct., VT 05001, USA
Phone: +1-802-296-2321, FAX: +1-802-296-2325, E-mail: obd@conceptsnrec.com
[2] MAN Turbomaschinen AG, Steinbrinkstrasse 1, D-46145 Oberhausen, Germany

ABSTRACT

A new reduced order through-flow analysis system for the preliminary design of axial turbomachines is presented. It has flexible models for losses, deviation, blockage, etc., uses real gas/liquid thermodynamics and handles flow and geometry at three spanwise locations. It is applicable to both compressors and turbines of either subsonic or supersonic flow type. The essential features of the system, including a comparison of its predictions with test data, are presented in the paper.

NOMENCLATURE

C	Absolute velocity	p	Pressure
Ch	Static enthalpy rise coefficient, $(h_2-h_1)/(h0_{1rel}-h_1)$	$P0$	Total pressure
		P	Power
		Pr	Pressure ratio
Co	Isentropic stage velocity	U	rotation velocity
		W	relative velocity
f	Function	ρ	Density
h	Enthalpy	ω	Total pressure loss coefficient
$h0$	Total enthalpy	δ	Deviation
i	Incidence	ξ	Kinetic energy loss coefficient, $(h_2-h_{2i})/(h0_{2rel}-h_{2i})$
K	Constant		
m	Mass flow	η	Adiabatic efficiency
M	Mach number	Ψ	Pressure rise coefficient, $\Delta p/(\rho U^2/2)$
N	Rotational speed		
		ϕ	Flow coefficient, w_m/U

Subscripts, superscripts:

*	design point, optimum value
1, 2	inlet, exit of the passage, respectfully
I	isentropic process
icc, ecc, ui	conditions of initial choking, established choking and unique incidence limitation
max, max_Koch	maximum value (stall), value by Koch correlation, respectfully
P	passage loss
Ref	normalized to the standard inlet conditions
rel	relative (rotating) frame of reference
tt,ts	total-to-total, total-to-static

INTRODUCTION

In the gas turbine design or rocket motor, the meanline analysis lays foundation of the engine, determines the cycle, meridional gas path configuration, number of stages, and stage work distribution. Despite the critical importance, meanline analysis systems used today have restrictions, limiting the scope of preliminary design optimization.

With the introduction of three-dimensional blade geometry and non-uniform spanwise aerodynamic loading, the traditional meanline analysis system is less capable of predicting correct passage areas, flow, and performance of the machine. Typically, it is restricted to a specific machine type, turbine or compressor in a single shaft configuration. Flow is often modeled using ideal, semi-perfect gas or incompressible fluid formulation, causing serious errors for real gases, media with phase change, and compressible liquids, such as liquid hydrogen.

Recognizing these shortcomings, Concepts NREC initiated development of a new system in 1996, with the first production release made in 1998. New features and improvements have continued to evolve since then.

DESCRIPTION OF THE SYSTEM

The following major features are incorporated in the new performance analysis system for axial flow machines.

The problems associated with highly three-dimensional airfoil geometry and flow patterns are dealt with by defining the airfoil geometry and solving flow along hub, mean radius, and tip streamlines, using a reduced-order radial equilibrium principle. Flux balancing is ensured by integration of all conservation properties from hub to tip, between inlet and exit of each modeled passage.

The machine is defined by a sequence of stages and components of arbitrary type (compressor or turbine); each component (blade row) can be either acceleration or deceleration cascade during normal mode of operation, rotating or stationary, with individual shaft speed and selection of loss and deviation models. Such representation of the machine eliminates limitations in mixed compressor-turbine multiple shaft configurations.

Out of several implemented operational modes, the following two analysis modes are most useful. The first one requires mass flow at inlet of the machine as input. This mode utilizes a fast component marching solution from inlet to exit of the machine and is useful for a subsonic flow analysis, but it is inappropriate for choked flow machines. The other mode requires pressure ratio of the whole module as input. This second mode is suitable for analysis of subsonic as well as supersonic flow machines, including those with choking at multiple locations, not known in advance. Multiple choking is supported with concurrent limitations, due to sonic throat or supersonic inlet (Unique Incidence Limitation). The operational basis of the second mode is a generic Broyden solution procedure (Press et al., 1992), coupled with the flow conservation equations. Reconfigurable lists of iterative variables and targets are used to formulate a specific task to the solver. During a run, the solver iterates variables to balance the conservation equations and to meet the established targets for all components, stages, and machine.

The structure of the solver was developed to separate the flow

analysis from the geometry, thermodynamic, and loss models. The result of the separation is a generic aerodynamic solver of reduced order through-flow quality. It accepts geometric data for areas, locations, and spatial directions at inlet, throat, and exit of each blade row from component-specific models. Thermodynamic properties and losses are computed from separate interchangeable models. New models for losses, media, and geometry can be quickly added using the established interfaces, without changes in the solver core.

Loss models are replaceable and their components are reconfigurable. Various loss-modeling options are provided to improve prediction accuracy for specific geometry, flow type, and technological base. These options are, in the order of increasing sensitivity: spanwise loss and deviation profiles, interchangeable loss component models, correction coefficient for overall loss, correction coefficients for individual loss factors, and user-specified coefficients applied in loss correlations. Both aero and parasitic losses, associated with disc friction, wetness, partial admission, and effects of bleed or flow injection, are calculated for each component of the machine. Simplified models of injections and bleeds for flow and heat, blade heating and cooling are supported on casing and blade surfaces.

All essential thermodynamic operations are implemented using non-degenerative combinations of real gas/liquid thermodynamic properties, such as enthalpy and pressure, or pressure and entropy, thus, excluding the use of pressure and temperature combination. This approach provides a single-value thermodynamic solution at any phase state of the media – dry, condensing or evaporating gases, mixtures of various chemical compositions, compressible or incompressible liquids. NASA GASP, ASME steam and D. B. Robinson real-gas libraries, are integrated into the solver to handle a wide variety of media including hydrocarbons, refrigerants and their mixtures.

The above capabilities improve flexibility of the system and reduce cost of development and support, by eliminating repetitive coding and allowing extremely high levels of model and feature sharing across different types of machines.

Predictive accuracy is of paramount importance for any design system, which depends on the selection of the preferred loss, deviation and blockage correlations. The standard loss systems implemented for turbines and compressors will now be discussed.

Compressor Loss System

The standard loss system for compressors is based on a model, described in Koch & Smith (1975) and Koch (1981), which uses correlations for profile, end-wall, shock and incidence loss components, end wall blockage, deviation, and a specialized model for stall conditions. Corrections for NACA, DCA, and MCA blade profiles are built in the systems.

The new system follows a strict component-based approach, which conflicts with the equivalent diffuser analogy for a whole stage in the original stall (Koch, 1981) and end-wall loss models. Each blade row is subjected to a direct diffuser analogy and evaluation of stall limit, which required adjustments in the correspondent correlations, given in Figures 8 and 10 of Koch (1981). The corrections were quantified to satisfy test results for a reference compressor stage.

The modified Koch model for stall appears to be satisfactory at design point operation. However, in some cases for off-design operation, this model (coupled with a end-wall blockage effect on exit pressure) showed progressive diminishing of the predicted stalling mass flow with the mass flow reduction at passage inlet. To avoid this problem, a further correction was applied to the maximum static enthalpy rise coefficient Ch_{max_Koch} in the correspondent amount of unrecoverable enthalpy loss Δh_{inc_loss} due to off-design operation.

$$Ch_{max} = Ch_{max\_Koch} - \Delta h_{inc\_loss}/(h0_{1\,rel} - h_1) \qquad (1)$$

This correction provides rapid deterioration of the maximum stalling capability with increase in flow incidence. The end-wall effects, the primary reason for stall in the Koch model, and the non-optimum flow incidence effects are, thus, combined in one stall criterion.

With individual stall evaluations for rotors and stators, the dynamic pressure/enthalpy factor for rotors was automatically incorporated, in addition to stator elements. This factor is introduced by Koch (1981) to account for the effect of distorted velocity triangles on maximum stalling capability.

Other loss models or their components reported by Lieblein (1960), Hirsch and Denton (AGARD, 1981), Wright and Miller (1991) are available and can be used to match specific technology and to check design sensitivity.

Turbine Loss System

The primary loss prediction system for turbines is based upon the combined correlations of several highly respected investigators: Ainley and Mathieson (1951), Dunham and Came (1970), Kacker and Okapuu (1981), and Moustapha, Kacker, and Tremblay (1990). The model is extended to operate at high supersonic flows by imposing smoothed limits on correction functions using the inlet Mach number.

Similar to compressors, overall losses are modeled by combining losses from various sources for each blade row. Individual blade loss components are assessed for profile, secondary, leakage, trailing edge, and shock losses. Rotating components also consider parasitic losses due to disk friction, partial admission, and wetness.

Handling Choking Flows

A special model is implemented to handle choking flow at the design and off-design conditions for convergent and convergent-divergent bladed passages. Two reference conditions for pressure at the exit of the choked passage are introduced. The first one, Initial Choking Condition (ICC), corresponds to a barely choked flow with a subsonic flow downstream of the choked location. The second condition is the Established Choking Condition (ECC), corresponding to a choked flow with full supersonic expansion within the passage geometry, where exit shock wave is weakened or cancelled. At these operating conditions the passage losses reach a minimum for a wide variety of typical geometries, as reported elsewhere, for example Okapuu (1987) and Deich (1984).

Condition ICC is computed by finding a pressure at subsonic exit for the choked mass flow, using deviation and loss predicted by conventional correlations for subsonic flow. Since shock effects on loss are minimized, deviation and loss at ECC can be assumed to be of the same magnitude as those at ICC. If no other information is available, this assumption provides a simple way to estimate ECC by computing the pressure at the supersonic exit of the passage at the specified loss, deviation, and choking mass flow. The property of minimum loss at ICC and ECC make these reference conditions useful for preliminary design optimization.

Test data demonstrate that in the transonic domain $p_{ecc} < p_{exit} < p_{icc}$, the choked flow experiences quite a complex change in loss and deviation, as is shown by shaded areas in Fig 1.
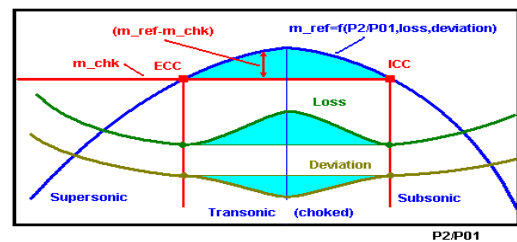

Figure 1. Dependency of passage mass flow, loss and deviation from pressure ratio.

In order to model losses and deviation in this domain, custom models are often considered. These models are either loss

correlations of test results of specific blade profiles (Chen, 1987), or semi-analytical models for compression-expansion wave structures, that require more geometry details at passage exit (Martelli et al. 1985). Once loss (or flow angle) is established, flow angle (or loss) immediately follows from the continuity equation. During a preliminary analysis, the detailed geometry is not available and a-priori knowledge of passage-specific transonic loss correlations is problematic, therefore, such models were ruled out from consideration in the system.

Instead, another approach was tried to predict cumulative shock loss (ξ_{sh}) as a function of difference between the reference mass flow m_{ref}, computed for loss and deviation frozen at ICC condition (line for m_ref in Figure 1), and choked mass flow m_{chk}, (horizontal line for m_chk):

$$\xi_{sh} = f_{\xi}(m_{ref} - m_{chk}) \tag{2}$$

Once the loss is defined, the deviation is computed to fully satisfy choked mass flow balance. The choked mass flow, required in this model, can be predicted quite accurately for a passage area at throat location, which is always available during preliminary design.

In this system concurrent operation of two choked flow conditions is allowed. These two conditions are sonic flow at throat of the passage, and Unique Incidence Limitation at supersonic inlet. The most restrictive of these choking limits defines ICC and ECC conditions, affecting loss and deviation in the transonic region.

The model appears to produce very sensible predictions for passages of convergent and convergent-divergent geometry in a wide range of operational conditions, as shown in Figure 2.
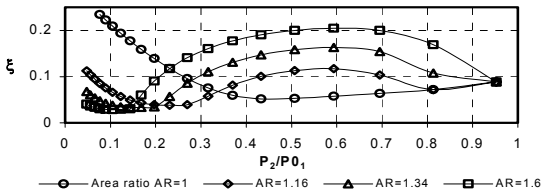

Figure 2. Cumulative loss in a passage vs. varied pressure at exit and exit area-to-throat ratio.

Based on the possible flow conditions at inlet and exit of a generic passage and flow restriction at the choked location, certain rules are implemented in the system of how to handle computations for deviation and loss, which are given in Table 1.

Table 1. Map for loss and deviation handling in a generic passage

Configuration	Condition		Loss	Devi-ation	Inlet Shock
Sb-Sb-NChk	$M < m_{chk} < m_{ui}$	$p_2 > p_{icc}$	Crl	Crl	-
Sb-Ts-THChk	$M = m_{chk} < m_{ui}$	$p_{ecc} < p_{out} < p_{icc}$	U	U	-
Sb-Su-THChk	$M = m_{chk} < m_{ui}$	$p_{out} < p_{ecc}$	Crl	Cnt	-
Su-Sb-NChk	$M < m_{chk} < m_{ui}$	$p_{out} > p_{icc}$	Crl	Crl	Yes
Su-Ts-THChk	$M = m_{chk} < m_{ui}$	$p_{ecc} < p_{out} < p_{icc}$	U	U	Yes
Su-Su-THChk	$M = m_{chk} < m_{ui}$	$p_{out} < p_{ecc}$	Crl	Cnt	Yes
Su-Ts-UIChk	$M = m_{ui} < m_{chk}$	$p_{ecc} < p_{out} < p_{icc}$	U	U	Yes
Su-Su--UIChk	$M = m_{ui} < m_{chk}$	$p_{out} < p_{ecc}$	Crl	Cnt	Yes

Configuration: [Inlet]-[Exit]-[Choking]
[Inlet], [Exit]: Su-supersonic, Ts-transonic, Sb-subsonic
[Choking]: NChk-no choking, THChk-choking at throat, UIChk-choking at supersonic inlet (Unique incidence limitation)
Loss, Deviation: Crl-compute from a correlation, Cnt-compute from continuity eqn, U-compute from continuity eqn using function, linking loss and deviation

The table provides a generic basis of how to solve subsonic and supersonic flow in a sequence of turbine and compressor components. It complements flow configuration analysis for a turbine stage (Meauze and Formaux, 1987).

When the flow is choked and supersonic at exit, the passage loss is complemented by additional shock penalty, using the following correlation:

$$\frac{\omega_p^*}{\omega_p} = 1 + 49.5(M_{2rel} - M_{2rel\_ecc})^3 + 3.3(M_{2rel} - M_{2rel\_ecc})^2 \tag{3}$$

At $M_{2rel\_ecc} = 1$ it agrees with the correlation suggested by Came (1995). Also, an additional loss correction is introduced beyond the condition of limit loading of an over-expanded supersonic flow in order to satisfy condition of the fixed tangential velocity at the passage exit.

COMPRESSOR PERFORMANCE PREDICTION

The results from a number of sample test cases will now be discussed.

Rotor of a Mixed Flow Supersonic Compressor (Case 1)

This design of a fully supersonic mixed flow rotor is well suited to test the model predictions for fully choked compressor components. The rotor tests were completed in a closed loop using refrigerant R113 (Mönig et al. 1993). The real geometry utilizes aerodynamic blade profiles and S-shaped contours at hub and tip with slightly non-axial exit. The last two features are not fully simulated in the system, because they are typically considered at later phases of compressor design. The case was set for DB Robinson real gas R113 properties and standard Koch & Smith model with Concepts NREC corrections. The Lieblein model for optimum incidence was preferred over the default Lieblein-AGARD model, since the latter showed unreasonable results in the operating range of $M_1 = 1.2$-1.7. Because of choked flow, all computations were done using analysis mode with given pressure ratio. The test and predicted results are compared in Figures 3 and 4, and Table 2.

Table 2. Rotor performance at design point Pr_{tt}=5.98, 14,000 rpm.

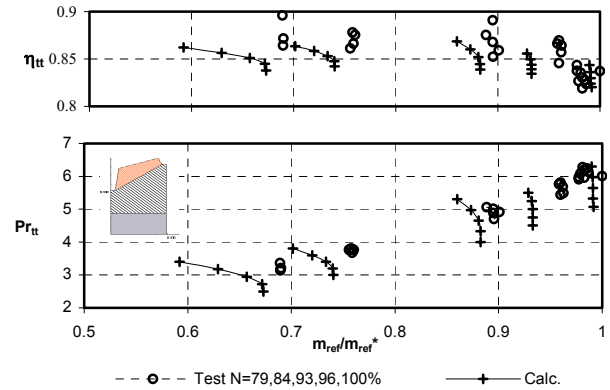| Parameter	Design Target	Test	Prediction	% Error
η_{tt}	~0.837	~0.82..0.83	0.836	<2%
m, kg/sec	16.8	~16.46	16.64	<1.5%

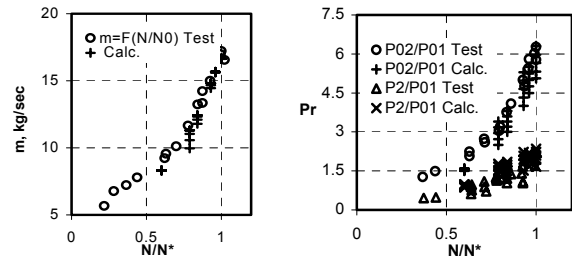**Figure 3.** Case 1, Supersonic rotor, performance map.

Figure 4. Case 1, Supersonic rotor, predicted mass flow and pressure ratio vs. rotation speed.

The results are in satisfactory agreement by magnitude and trends with the test data. The difference is attributable to the underestimated exit area due to the above-mentioned geometric features.

Two-Stage Transonic Compressor (Case 2)

The two-stage fan operates at an inlet tip Mach number of 1.49 and 442 m/s speed. The design targets are shown in Figure 6. The tests demonstrated 85.7% adiabatic efficiency, which is higher than the design target, with 10% stall margin at the design speed. Rotors and stators are MCA airfoil sections, as described in Ruggeri et al. (1974).

The stall operational limits at each constant speed line were determined by the following criteria: (a) $Ch > Ch_{max}$, for rotors, (b) $d(Pr_{tt})/d(m) = 0$, (c) $d(\Psi_{ts})/d(m) = 0$ for a stage, and (d) no converged solution. The last condition can be considered as one of the stall criteria, because it reflects flow stability problems in a real machine.

Preliminary calculations showed underestimation in pressure loss in the low speed operation range. To improve loss prediction, a correction curve (Figure 5) was introduced. With this correction the fan performance is predicted reasonably well, including a transonic flow domain (Figure 6).
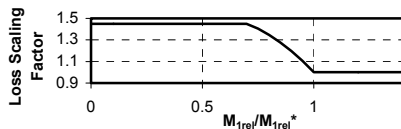

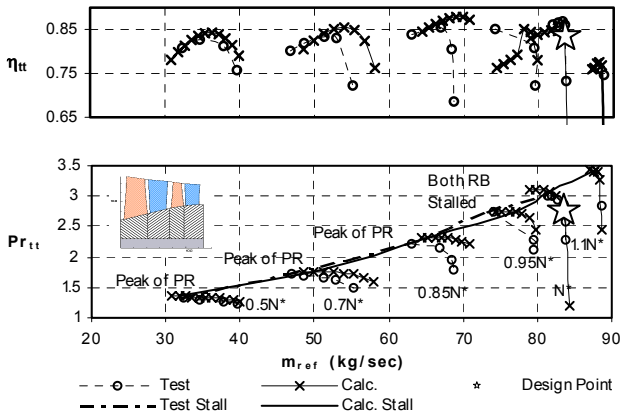**Figure 5.** Case 2, Loss correction curve for the two-stage fan case.

Figure 6. Case 2, Overall performance prediction of two-stage transonic fan.
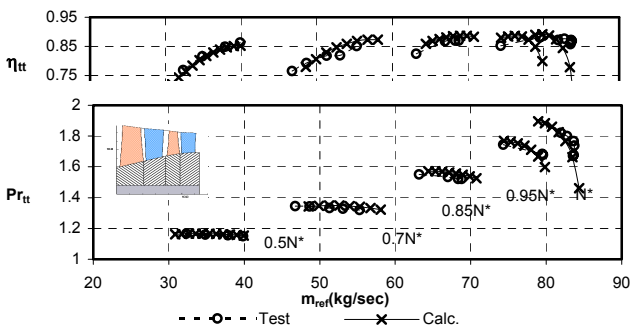

Figure 7. Case 2, Performance of the first stage of two-stage transonic fan

The largest difference of the predicted efficiency is 2.4% at 85% speed for peak efficiency point and -4.2% at 90% speed for the stalling pressure ratio point. The predicted efficiency and choke flow for speeds above 95% agree very well with the test data. The specific reason of stall criteria violation is shown in Figure 6 for every speed. Performance of the first stage, Figure 7, is also predicted well.

NASA 3S1 and 3S2 Subsonic Three-Stage Compressors (Case 3)

These two subsonic compressors have similar design features except for their blade aspect ratio: 0.81 for 3S1 and 1.22 for 3S2. Such stages are typical for rear stages of a highly loaded multistage compressor. The design targets and test results are shown in Figure 8 (Burdsall et al. 1979 and Behlke et al. 1979).

The standard Koch & Smith loss system with Concepts NREC corrections was used for this analysis. Scaling factor of 2.45 for blockage was introduced for stators, to provide better agreement with test data. The required blockage increase could be due to large boundary layer separation occurring in stators of compressors with conventional blading. The stall criteria were the same as that defined in Case 2. The predicted and measured performance is shown in Figure 8.
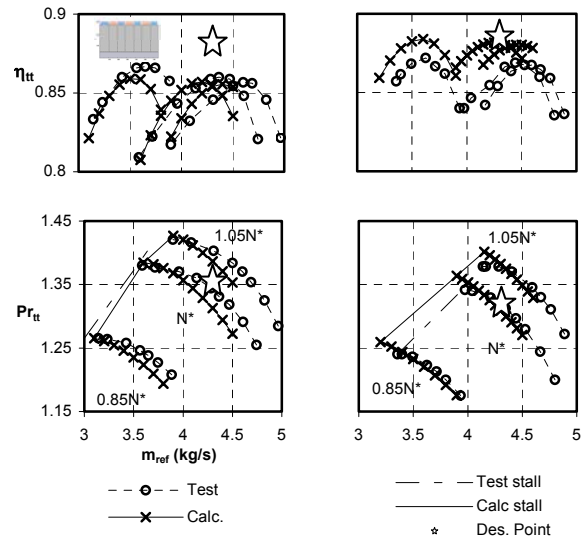

Figure 8. Case 3, NASA 3S1 (left) and NASA 3S2 (right) compressor performance maps.

The stall conditions in these calculations were limited by the unconverged solution for both 3S1 and 3S2 at every rotational speed. The predicted performance and stall lines follow the test results reasonably well. The maximum difference between calculated and measured peak efficiency is -0.7% at 85% speed for 3S1, +1.3% at all speeds for 3S2. The difference becomes larger on the choking side of the operating ranges. The aspect ratio effect on performance is captured well, though it is stronger than in the tests data. This may indicate that the aspect ratio correlation is too severe. The maximum difference for the predicted pressure ratio on the stall line is -1.5% for 3S1, and 3.2% for 3S2, both observed at 85% design speed.

Stage pressure rise characteristics at 100% design speed are shown in Figure 9. In this figure, the flow coefficient and the static pressure rise coefficient are calculated in the same way as for test data, described in Behlke et al. (1979).
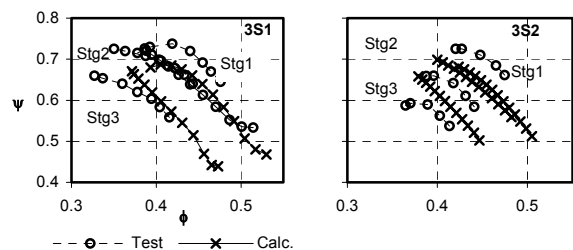

Figure 9. Case 3, NASA 3S1 (left) and 3S2 (right) compressors, pressure rise coefficient vs. flow coefficient.

Pressure rise characteristics of each stage of the 3S1 compressor (Figure 9 left) are predicted well, including trends for off peak operation of Stage 1, and negatively sloped stable characteristics of Stages 2 and 3. Usually, a compressor loses stability when the slope of $\phi-\psi$ characteristic becomes near zero. For this reason and according to the test data, Stage 1 can be considered to initiate the stall. Generally, unsteady calculations like Nakano et al. (1999, 2002) are needed to obtain the overall instability point of a multistage compressor. In this case, however, the boundary of unconverged solutions agrees well with the overall stall line. It is possible, that steady analysis with proper blade performance models, covering stalled domain, may still be capable of predicting the instability operating point of a multistage compressor.

The test data for 3S2 compressor (Figure 9 right) show that all three stages reach zero slope at compressor stall, thus, stall is initiated by near simultaneous stability loss by all stages. Calculations do not show such peaked characteristics, instead unconverged solutions, indicating unstable operation, are observed for Stages 2 and 3 beyond the maximum pressure rise, plotted in the figure. The predicted stability limits are similar to the test results. The slope of the calculated characteristics on the stall side in Figure 9 slightly exceeds the ones observed in the test data.

Four-Stage Transonic BBC/SULZER Compressor (Case 4)

This test case is reported in AGARD-AR 175 (Hirsch and Denton, 1981) and is known as BBC/SULZER compressor with four stages and a design pressure ratio of 3.05 at 15,000 rpm. Except for the IGV, all blade rows are built of DCA-profiles.

Prior to this test case, a validation effort was done for a single stage case transonic compressor E/CO-4 (Fottner, 1990) with MCA blades for rotor. In that case, the built-in loss and deviation correlations have proved to be inadequate to accurately predict the first rotor characteristics. They were modified based on calibrated 2D and 3D CFD computations, using the following corrections:

$$\delta - \delta^* = k_1 \cdot M_1 + k_2 \quad (4)$$
$$\omega - \omega^* = k_3 \cdot (i - i^*)^2$$

The constants $k_1 - k_3$ were determined for several transonic MCA profiles, correlated to cover a wide range of applications and introduced in the system via so-called *.ulc files, reserved for users who want to implement custom correlations. For the NACA65-stator, the standard correlations were applied after they were validated against 2D CFD-runs. With these corrections, the calculations showed excellent agreement in pressure ratio with test data and results of a modified calibrated version of Denton multistage solver. The calculated efficiency did not match the test data by magnitude, but the trends and position of the maximum efficiency were reproduced correctly. Standard rules generally do not apply in the modeling of transonic flow, and the described approach is common in the design of first transonic stages. The effect of shocks on overall loss is still a matter of research for transonic flow in meanline or through flow solvers (Boyer et.al. 2002).
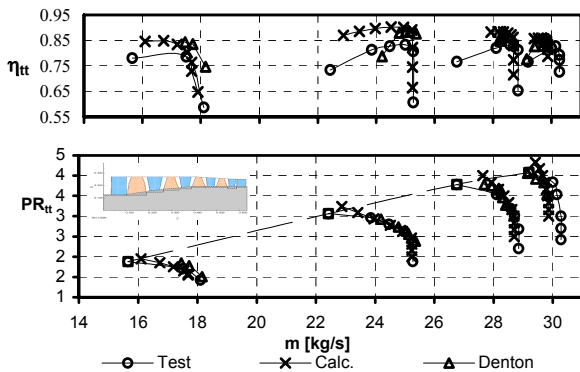
Figure 10. Case 4, BBC/SULZER compressor test case.

In the case of the four-stage compressor the loss and deviation correlations have been modified in the manner described above. The predicted performance maps are shown in Figure 10.

The agreement with experiments is quite encouraging. In comparison with the results of Denton's solver the characteristics are steeper for the high inlet Mach number cases at higher rotational speeds.

NASA/GEAE E[3] 10-Stage Compressor (Case 5)

The 10-stage high-pressure-compressor (HPC) has transonic stages in the front and subsonic stages in the rear. The design relative inlet Mach number is 1.35 at tip of the first rotor, the design targets are shown in Figure 11. The detailed design and test results are reported in Holloway et al. (1982) and Cline et al. (1985).

The same loss correction curve introduced in Case 2 was used for the transonic blades in the front stages. Blockage factor up to 3.5 was applied toward rear stages, which is consistent with the correction applied in Case 3. In front stages the end wall blockage was reduced by a factor of 0.5. Stall criteria and loss models were the same as in Case 3, except that the max limit and slope of end wall loss model were relaxed in the extrapolation domain, where the Koch stall criterion is violated.

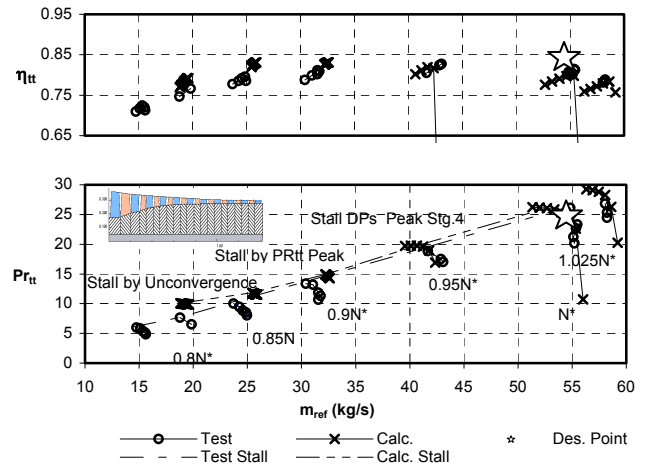The calculated performance and test data are shown in Figure 11.

Figure 11. Case 5, NASA/GE E[3] 10 stage compressor.

The predictions follow the test data very well, especially above 85% design speed. The maximum difference of the predicted peak efficiency is +2.2% at 90% speed. The difference at 100% speed is -1.5% in comparison with the measured data. It would increase to -4.1% with a 2.6% correction suggested by Cline et al. (1985). The maximum difference of pressure ratio on the stall line above 85% speed is +3.2% at 95% speed. The choked flow is predicted very well at high speeds above 90%. The code predicts that stall initiates at Stage 4 at high-speeds, while in a multistage compressor stall usually initiates from rear stages. Similar performance results were obtained using the loss adjustments similar to Case 4 and for the Denton code.

Summary of Compressor Validations

The above comparisons indicate that the predictions are generally in good agreement with the test data and results of more sophisticated solvers. Even overall performance of a ten-stage highly loaded compressor can be predicted within a tight error band. However, some of the built-in models require further modifications. The magnitude of the applied modifications appears to be largely design specific, with consistent trends for end-wall blockage of high hub/tip ratio blade rows, and losses for transonic rotors at partial speeds. This implies that once the user establishes the set of loss model modifications, fit to the particular family of compressors and technology, the system becomes a solid tool for performance predictions of future designs of similar compressors.

User specified modifications of the built-in correlations allow model tuning to the specific applications.

Effects of spanwise loss and deviation distributions were not addressed in the discussed cases.
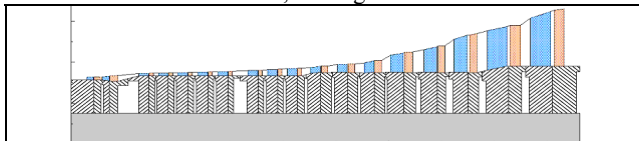
TURBINE PERFORMANCE PREDICTION

This system was developed to predict the many different types of axial turbine stages encountered in industry today: velocity-compound (Curtis) stages, partial admission impulse blades, convergent-divergent supersonic blades, high reaction gas turbine stages and low-pressure condensing stages, with additional features of flow inductions or extractions, moisture removal, cooling flows, and lashing wire losses.

The results from a number of sample test cases will now be discussed. These cases provide a rigorous validation of the system for a wide variety of turbine blade types and operating conditions.

Condensing Steam Turbine (Case 1)

Table 3 shows the flow path model for a 17-stage condensing steam turbine with three uncontrolled extractions. This turbine was designed and field-tested by Elliott Company for a waste to energy installation. The steam path consists of a partial admission inlet Curtis stage followed by 32 rows of alternating impulse-type nozzles and buckets that progress from high-pressure to low-pressure stages with corresponding low- to high-aspect ratio blades. Special features include: lashing wire losses and large wetness considerations for both thermodynamics and losses. All key performance parameters were predicted with good accuracy using standard loss models with no special corrections.

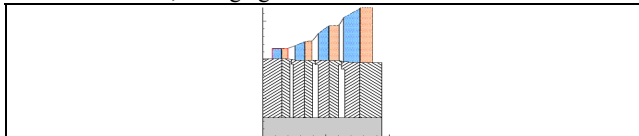**Table 3.** Case 1, 17-stage steam turbine.

Parameter	Units	Test Data	Prediction	% Difference
m	kg/sec	25.20	24.51	-2.7%
P	KW	23,449	23,054	-1.7%
Steam Rate	kg/kW-hr	3.87	3.83	-1.1%

*data courtesy of Elliott Company

Geothermal Steam Turbine (Case 2)

Table 4 shows the flow model for a four-stage geothermal steam turbine with saturated inlet conditions. This case provided a demanding assessment of convergence and predictive abilities for multiple-choked, transonic blade rows operating with high moisture losses. Again, all key performance parameters were predicted with high accuracy using standard loss models with no special corrections.

Table 4. Case 2, 4-stage geothermal turbine.

Parameter	Units	Design Data	Prediction	% Difference
m	kg/sec	26.71	26.67	-0.2%
P	KW	10364	10372	+0.1%
Steam Rate	kg/kW-hr	9.28	9.26	-0.2%

*data courtesy of Elliott Company

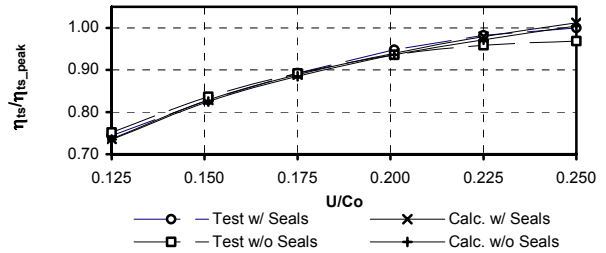### Partial-Admission Curtis Stage (Cases 3A & 3B)

The third case is a 44% admission Curtis stage designed and tested by Elliott Company under choking conditions with transonic flow occurring in the rotor. Figure 12 shows that the stage efficiency was accurately predicted over a wide range of velocity ratios, both with and without bucket tip seals. The flow rate was predicted within 2.2% of the reported flow data.
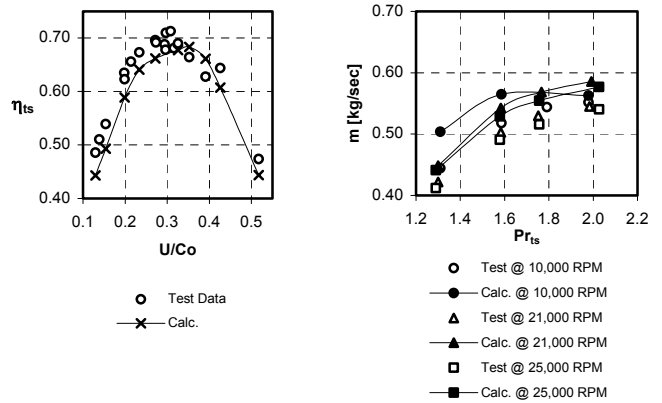
NASA Partial-Admission Turbine (Case 4)

The fourth test case is a 34% admission, two-stage turbine that was tested under subsonic conditions (Richter, 1992). Figure 13 shows that efficiency predictions follow the test data quite well.

Several different circumferential orientations of the second stage 45% admission arc were investigated during the test program to find the optimum position. Figure 13 test data is for the optimum nozzle orientation, while other orientations resulted in three points to ten points lower efficiency depending on velocity ratio. The predictions agree better with these less optimum orientations at the lower velocity ratios.

Figure 12. Cases 3A and 3B - Partial admission Curtis stage efficiency with and without tip seals (courtesy of Elliott Company).

Figure 13. Case 4, NASA partial admission turbine efficiency and flow rate.

Also, the amount of partial admission fan out between blade rows had to be estimated since it is unknown. A linear increase of downstream stage admission with velocity ratio was found to result in the best match with measured efficiency data.

Finally, Figure 13 shows that flow predictions were generally 6% to 7% higher than measured values from test but followed the pressure ratio and speed trends quite well.

Supersonic Turbines (Cases 5 & 6)

Further comparisons were done for two small supersonic turbines with design total-to-static pressure ratio of 6 and 88. Geometry and test results are presented by Verneau (1987) and Kurzrock (1989). These test cases provide a rigorous demonstration of the system to handle highly supersonic designs, which are subject to multiple choking (nozzle and rotor) and concurrent choking at throat and inlet (due to Unique Incidence Limitation) in the supersonic rotors. Calculations at design operating point for Case 5 show that rotor choking occurs at the throat location. In Case 6, however, Unique Incidence Limitation at the rotor inlet appears to be more restrictive, than choking at the throat.

Convergent-divergent nozzle case (Case 5)

This case represents an exhaust recovery low power turbine that was designed for a total-to-static pressure ratio of 5.15 while operating on refrigerant R113 with 39.4% admission (Verneau, 1987). Convergent-divergent bladed nozzles (design

Mach No. = 1.76) have practically no flow turning in the passage, which was the reason to reduce the standard secondary flow loss in the nozzle by 80% for calculations. Frolov's et al. (1972) partial admission model was preferred, since it has corrections for lower admissions. Design point efficiency and reaction predictions matched test data within 1%. The average deviation for off-design efficiency was only 1.1% over the full range of test data (see Figure 14).
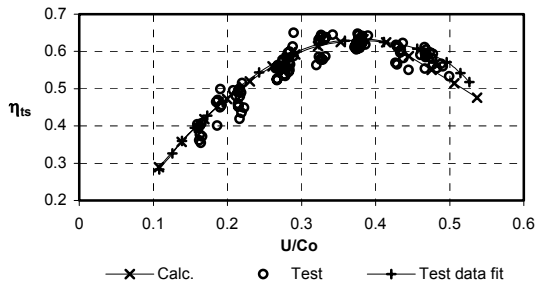

Figure 14. Case 5, Low power supersonic partial admission turbine ($Pr_{ts} = 5.15$).

Axisymmetric (drilled) nozzles (Case 6)

The second turbine was designed for $PR_{ts} = 88$ and was tested in a CO_2 rig (Kurzrock, 1989). It has drilled (round) supersonic nozzles (design exit Mach~3) with no flow turning in the passage and elliptic exit opening. To accommodate this geometry, the standard loss model for secondary flow was disabled and an 88% admission arc was set for correct exit area computations. Incomplete admission arc generates additional end-segment and ventilation loss, approximating effects of highly non-uniform flow from the elliptic openings of the nozzle ring. Predictions closely follow the test data at both design and off-design conditions, as shown in Figure 15, at both $PR_{ts} = 33$ and 88.
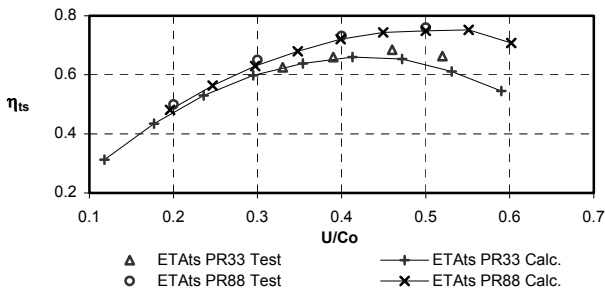

Figure 15. Case 6, Supersonic turbine efficiency ($Pr_{ts}=88$).

NASA /Pratt & Whitney High-Pressure E^3 Turbine (Case 7)

The Pratt & Whitney (P&W) design of a high-pressure turbine was selected to verify the code predictions for higher reaction blades. This is a highly loaded single stage axial turbine designed for the NASA/P&W Energy Efficient Engine (E^3) as referenced in Crow et al. (1980), Thulin et al. (1982), NASA CR-159487 (1978), Bryce (1985). The scaled turbine tests were carried out in an existing P&W turbine rig in which boosted air was used to drive the uncooled test turbine.

Efficiency comparisons for 100% design speed (left) and 80% and 107% off-design speeds (right) show that calculations closely agree with the test data at both design and off-design pressure ratio and speeds (Figure 16). In fact, the efficiency difference is less than one half point at the design pressure ratio of about 4.0, for all three speeds, and about one point or less at the most extreme off-design pressure ratio of about 5.5 (and design speed). Calculations and test results both show "an efficiency dip" in the transonic flow regime. The transonic flow regime is defined as a flow condition between ICC and ECC conditions discussed above. The test supports validity of the implemented models to handle losses in choked passages.
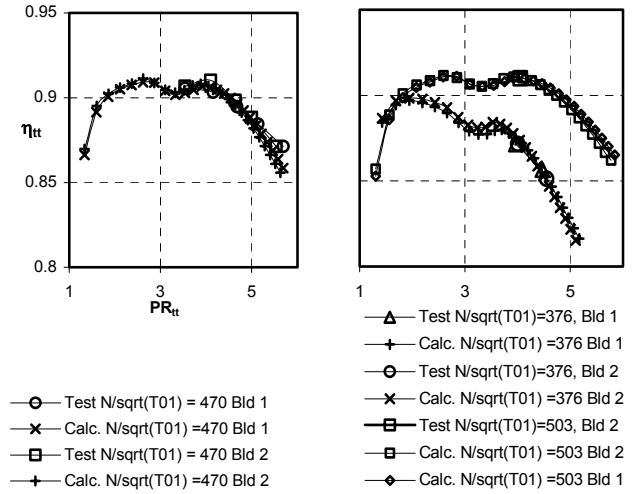

Figure 16. Case 7, NASA/PWA's E^3 HP turbine performance at 100%(left)and 80%,107% (right) design speed.

Summary of Turbine Validations

Table 5 provides a summary of the validation results for the above seven test cases. These comparisons illustrate a rigorous validation of the accuracy for a wide variety of turbine blade types and operating conditions. Both design and far off-design calculations were compared with test data under demanding circumstances: high moisture, partial admission, supersonic flow (at both blade inlet and exit), and multiple choked rows.

From these results we can conclude that the system is highly capable of accurately predicting the performance characteristics of many different types of axial turbine stages encountered in industry today.

Table 5. Summary of turbine test cases

Case No.	Source	Application	Features	No. Stages	Stage Pressure Ratio Range	Power Output, kW	Prediction Accuracy Design Point	Prediction Accuracy Full Range [**]
1	Elliott*	Condensing steam turbine	W	17	1.2 – 3.2	23,449	-1.1 %	- - -
2	Elliott*	Geothermal turbine	M, T, W	4	1.8 - 4.5	10,364	-0.4 %	- - -
3A	Elliott*	Curtis stage with seals	P, T	1	3.2	720	+1.2 %	0.5 %
3B	Elliott*	Curtis stage without seals	P, T	1	3.2	715	+3.7 %	1.1 %
4	Richter (1992)	Small impulse turbine	P	2	1.1 – 1.5	15	+3.0 %	2.3 %
5	Verneau (1987)	Exhaust recovery turbine	M, P, S	1	6.0	3	-0.6 %	1.1%
6	Kurzrock (1989)	Aerospace accessory power turbine	A, M, P, S	1	33 & 88	48	-0.9 %	2.9%
7	***	Energy efficient engine, HP turbine	M, T	1	3.5 – 5.7	2,456	-0.4 %	0.4%

*test data courtesy of Elliott Company
**FULL RANGE is average prediction error for efficiency over full range of reported test results.
*** Source is: Crow et al. (1980), Thulin et al. (1982), NASA CR-159487 (1978), Bryce (1985)
Features:
P = Partial admission   S = Supersonic flow (M > 2)   M = Multiple choked rows
W = Wet steam   T = Transonic flow (M < 2)   A = Axi-symmetric (drilled) nozzles

FUTURE DIRECTIONS

The case validation and loss model updates are in progress with further development of the system. The next logical step is to add capability to handle preliminary analysis of a complete gas turbine engine, in order to solve tasks of shaft and aerodynamic matching of compressor and turbine modules, estimating regions of stable operation, and overall engine performance. With some limitations, the current system already supports this functionality,

as shown in Figure 17. The system can also easily be extended to support axial and mixed flow geometries in one design. Adding effective modes for conceptual multistage design and custom stage design can be valuable to reduce the overall time for preliminary design.
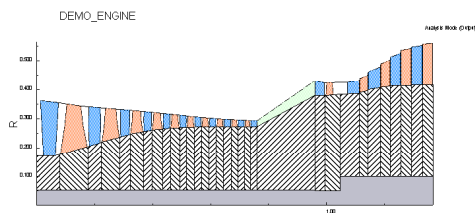

Figure 17. Demo setup of a gas turbine engine.

CONCLUSIONS

A very flexible and versatile preliminary analysis system was developed on the basis of reduced order through-flow modeling. Some modeling details were discussed and 12 validation cases were presented.

The compressor validation cases demonstrate that the system generally agrees well with the test data. However, some of the built-in models need to be modified to get the best possible match with the test data. The trends of the modifications appear to be consistent throughout the considered cases.

The turbine validation cases show that the system generally agrees very well with the test data without any modifications to the built-in models.

In summary, the considered system is an effective performance analysis tool for the early phase of aerodynamic design of axial-flow compressors and turbines, and can be an ideal platform for a design optimization system.

ACKNOWLEDGMENT

REFERENCES

Press, W. H., Teukolsky, S. A., Veterling, W. T., Flannery, B. P., 1992, "Numerical Recipes in Fortran," Cambridge University Press, New York, pp. 382-385.

Ainley, D. G., and Mathieson, G. C. R., 1951, "A Method of Performance Estimation for Axial Flow Turbines," British ARC, R&M 2974.

Behlke, R. F., Burdsall, E. A., Canal Jr., E., and Korn, N. D., 1979, "Core Compressor Exit Stage Study II. Final Report," NASA CR-159812.

Boyer, K. M, 2002, "An Improved Streamline Curvature Approach for Off-Design Analysis of Transonic Axial Compression Systems," ASME-Paper GT-2002-30444.

Bryce, J. D., Litchfield, M. R., and Leversuch, N. P., 1985, "The Design, Performance and Analysis of a High Work Capacity Transonic Turbine," Trans. of ASME, Journal of Engineering for Gas Turbine and Power, October 1985.

Burdsall, E. A., Canal Jr., E., and Lyons, K. A., 1979, "Core Compressor Exit Stage Study: 1.Aerodynamic and Mechanical Design," NASA CR-15971.

Came, P. M., " Streamline Curvature Through-Flow Analysis of Axial Flow Turbines," VDI Berichte NR. 1185, 1995.

Chen, S., 1987, "A Loss Model for Transonic Flow Low Pressure Steam Turbine Blades," I. Mech. E. Paper C271/87, pp. 145-153.

Cline, S. J., Fesler, W., Liu H. S., Lovewell, R. C., and Shaffer, S. J., 1983, "Energy Efficient Engine, High Pressure Compressor Component Performance Report," NASA CR-168245.

Crow, D. E., Vanco, M. R., Welna, H., and Singer, I. D., 1980, "Results from Tests on a High Work Transonic Turbine for an Energy Efficient Engine," ASME Paper 80-GT-146.

Deich, M. E., Zaryankin, A. E., Gidrogazodinamika, Moscow, Energoatomizdat, 1984, pp. 310-31112.

Dunham, J., and Came, P. M., 1970, "Improvements to the Ainley/Mathieson Method of Turbine Performance Prediction," ASME, J. of Eng. for Power, pp. 252-256.

Fottner, L., 1990, "Test Cases for Computation of Internal Flows in Aero Engine Components: Test case E/CO-4," AGARD-AR-275, pp. 245-284.

Frolov, V. V. and Ignat'evskii, E. A., 1972, "Calculating The Windage Losses in a Turbine Stage," Teploenergetika, 19 (11), pp. 33-37.

Hirsch, Ch., Denton, J. D., 1981, "Through Flow Calculations in Axial Compressors," AGARD-AR-175, pp. 229-255.

Holloway, P. R., Knight, G. L., Koch, C. C., and Shaffer, S. J., 1982, "Energy Efficient Engine, High Pressure Compressor Detail Design Report," NASA CR-165558.

Kacker, S. C., and Okapuu, U., 1981, "A Meanline Prediction Method for Axial Flow Turbine Efficiency," ASME J. of Eng. for Power, Vol. 103, No. 1.

Koch C. C., Smith, L. H., 1975, "Loss Sources and Magnitudes in Axial Flow Compressors," Transactions of the ASME, Journal of Engineering for Power, 75-WA/GT-6.

Koch, C. C, 1981, "Stalling Pressure Rise Capability of Axial Flow Compressor Stages," Journal of Engineering for Power, Vol. 103, pp. 645-656.

Kurzrock, J. W., 1989, "Experimental Investigation of Supersonic Turbine Performance," ASME paper 89-GT-238.

Lieblein, S., 1960, "Incidence and Deviation- Angle Correlations for Compressor Cascades," Trans. of ASME, Journal of Basic Engineering, September, pp. 575-587.

Martelli, F., Boretti, A. A., 1985, "A Simple Procedure to Compute Losses in Transonic Turbine Cascade," ASME paper 85-GT-21.

Meauze, G., Formaux, A., 1987, "Numerical Simulation of Flows in Axial and Radial Turbomachines using Euler Solvers," VKI, lecture series 1987-07.

Mönig, R., Elmendorf, W., Gallus, H., 1993, "Design and Rotor Performance of a 5:1 Mixed-Flow Supersonic Compressor."

Moustapha, S. H., Kacker, S. C., and Tremblay, B., 1990, "An Improved Incidence Losses Prediction Method for Turbine Airfoils," ASME J. of Turbomachinery, Apr. 1990, pp. 267-276, ASME Paper 89-GT-284.

Nakano, T., Kodama, H., and Imanari, K., 1999, "Numerical Simulations of Instability Inception and Development in High-Speed Multistage Axial-Flow Compressors," ISABE paper, No.99-7228.

Nakano, T. and Kodama, H., 2002, "Numerical and Experimental Investigation of Instability Inception in a High-Speed Axial-Flow Compressor using Chaos Theory," AIAA 2002-4089.

Okapuu, U., 1987, "Aerodynamic Design of First Stage Turbines for Small Aeroengines," VKI, lecture series 1987-07, Journal of Turbomachinery, Vol. 115, pp. 565-57215.

Richter, P. G., 1992, "Design and Experimental Performance of a Two-Stage Partial Admission Turbine, Task B1./B.4.," NASA CR-179548.

Ruggeri, R. S. and Benser, W. A., 1974, "Performance of a Highly Loaded Two-Stage Axial-Flow Fan," NASA TMX-3076.

Thulin, R. D., Howe, D. C., and Singer, I. D., 1982, "Energy Efficient Engine High-Pressure Turbine Detailed Design Report," NASA CR-165608.

Verneau, A., 1987, "Supersonic Turbines for Organic Fluid Rankine Cycles from 3 to 130 KW," VKI, lecture series 1987-07.

Wright, P. I., Miller, D.C., 1991, "An Improved Compressor Prediction Model," paper C423/028, *Turbomachinery: Latest Developments in a Changing Scene*, Proc. I. Mech. E., 1991-3, pp. 69-75.